REPORT DOCUMENTATION PAGE

Form Approved
OMB NO. 0704-0188

1. AGENCY USE ONLY (Leave Blank)	2. REPORT DATE 11/27/00	3. REPORT TYPE AND DATES COVERED final, 3/01/99-2/29/00

4. TITLE AND SUBTITLE
Research Instrumentation for Photonic Bandgap Photonics

5. FUNDING NUMBERS

DAAD19-99-1-0021

6. AUTHOR(S)
John O'Brien

7. PERFORMING ORGANIZATION NAME(S) AND ADDRESS(ES)
University of Southern California
University Park,
Los Angeles, CA 90089-0271

8. PERFORMING ORGANIZATION REPORT NUMBER

9. SPONSORING / MONITORING AGENCY NAME(S) AND ADDRESS(ES)
U. S. Army Research Office
P.O. Box 12211
Research Triangle Park, NC 27709-2211

10. SPONSORING / MONITORING AGENCY REPORT NUMBER

ARO 39342.1-PH-RIP

11. SUPPLEMENTARY NOTES
The views, opinions and/or findings contained in this report are those of the author(s) and should not be construed as an official Department of the Army position, policy or decision, unless so designated by other documentation.

12 a. DISTRIBUTION / AVAILABILITY STATEMENT

Approved for public release; distribution unlimited.

12 b. DISTRIBUTION CODE

13. ABSTRACT (Maximum 200 words)

This program funded the purchase of a Sun Ultra 60 dual processor workstation and tunable laser modules from New Focus that complement our existing tunable diode laser and extend the tuning range from 1470 nm to 1620 nm. These were, and continue to be, used in our work on photonic crystal devices. In particular, the workstation has been used to calculate modes for the design of a single defect microcavity photonic crystal laser. We are also modeling and fabricating photonic bandgap waveguides. Here both the workstation and the tunable laser are to be used. In addition, they are also both a part of the work being done on superprism and super-dispersion structures that are under investigation in our lab.

DTIC QUALITY INSPECTED 4

20010117 095

14. SUBJECT TERMS			15. NUMBER OF PAGES 10
			16. PRICE CODE

17. SECURITY CLASSIFICATION OR REPORT UNCLASSIFIED	18. SECURITY CLASSIFICATION ON THIS PAGE UNCLASSIFIED	19. SECURITY CLASSIFICATION OF ABSTRACT UNCLASSIFIED	20. LIMITATION OF ABSTRACT UL

Final Report for Research Instrumentation for Photonic Bandgap Photonics

4. Statement of the Problem Studied

This program funded the purchase of a Sun Ultra 60 dual processor workstation and tunable laser modules from New Focus that complement our existing tunable diode laser and extend the tuning range from 1470 nm to 1620 nm. These were, and continue to be, used in our work in photonic crystal devices. In particular, the workstation has been used to calculate modes for the design of a single defect microcavity photonic crystal laser. We are also modeling and fabricating photonic bandgap waveguides. Here both the workstation and the tunable laser are to be used. In addition, they are also both a part of the work being done on superprism and super-dispersion structures that are under investigation in our lab.

Final Report for Research Instrumentation for Photonic Bandgap Photonics

5. Summary

This proposal was for a tunable laser and a workstation. These are important components in the work on two-dimensional photonic bandgap devices going on in my research group. The original proposal was intended for these two pieces of equipment to be used for photonic crystal waveguides and microcavity lasers. They have been used for these projects. In addition, since the time of the proposal, the work on photonic crystals in my group has broadened. We are also currently working on engineering the radiation pattern of these microcavity lasers and using the super-dispersion of photonic crystals to guide optical beams. In this report, I'll discuss the progress by research project. I'll start with the work on microcavities lasers.

We have demonstrated, in collaboration with Professors Scherer and Yariv at Caltech and Professor Dapkus here at USC a microcavity based on a single defect in a two-dimensional phot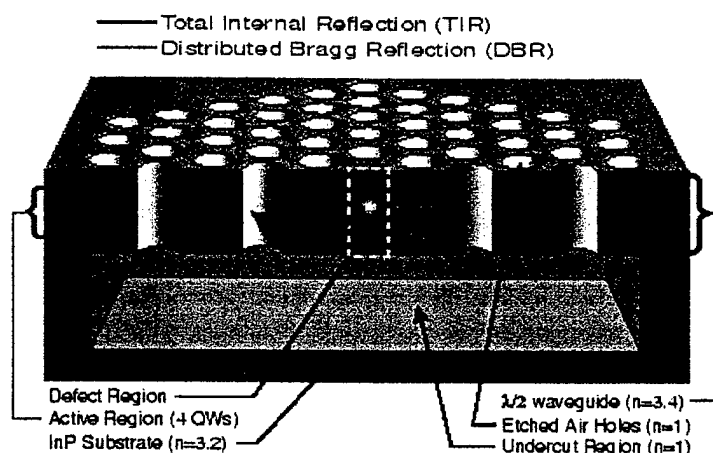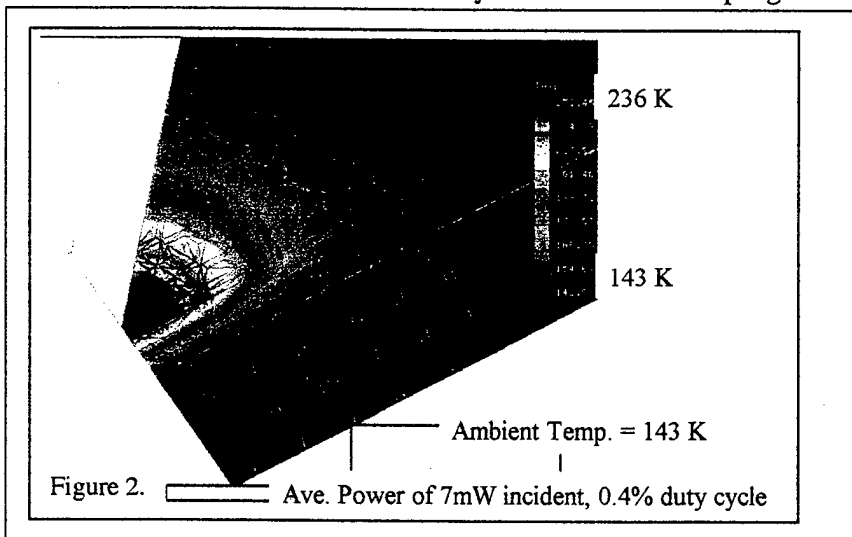onic crystal. The structure is shown in figure 1. The cavity consists of a 220 nm thick semiconductor membrane that contains 4 InGaAsP quantum wells. This membrane is formed by removing an underlying InP layer selectively using HCl. Before this semiconductor membrane is formed, a two-dimensional photonic crystal is defined into it using an electron-beam lithography step, followed

Figure 1.

by an ion beam mill, a reactive ion etch, and a chemically-assisted ion beam etch. This work has resulted in three publications to date [1-3]. The initial demonstration was done in pulsed operation at low temperature [1]. Subsequent work has led to room-temperature pulsed operation [2], and a demonstration of lithographically defined lasing wavelengths [3]. This last work demonstrated tuning from 1500 to 1625 nm from a single wafer by lithographically varying the lattice constant and the ratio of the hole radius to the lattice constant. Professor Dapkus and I are currently pursuing microcavities that will operate continuously at room temperature. The problem with the initial cavity is that it does not dissipate heat effectively. Shown below in figure 2 is a calculation of the temperature distribution in the photonic crystal microcavity. The figure shows one-sixth of the cavity. This calculation was done in my group using commercial software. Here the substrate is held at the temperature of the initial demonstration, 143 K. The membrane is heated by absorbing optical power and is about 100 degrees hotter than the substrate. In this calculation, the membrane is allowed to cool through conduction, convection, and radiation. This elevated temperature of the

membrane reduces the peak gain and makes it difficult to achieve continuous lasing. Therefore, we are working on an alternative structure. The new structure will be fusion bonded to a sapphire layer, which may eventually itself be bonded to a backside emitting VCSEL array for optical pumping. The sapphire will provide a thermally conductive substrate to conduct the heat as well as a reasonably low-index material for mode confinement. This work is funded by a DARPA STAB program. The sapphire, however, complicates the electromagnetic design of the cavity. Most importantly, the symmetry is broken so that there no longer exist purely even and odd modes. This rigorously eliminates the bandgap of the photonic crystal. Practically, the bandgap still exists if the waveguide is made thick enough. In this case, the semiconductor waveguide cladding is symmetric on each side of the quantum wells and thick enough so that the asymmetry is a small perturbation on the cavity mode. Shown below in figure 3 is a finite-difference time-domain calculation of the fields in a photonic bandgap cavity. The figure on the left has symmetric air cladding on the top and bottom. On the right, the top cladding is air and the bottom cladding is sapphire. This code was written by my students, and runs on the dual-processor Sun Ultra 60 workstation purchased under this program. As can be seen in the figure, the cavity on the right radiates preferentially into the high-index substrate. The calculated quality factor of the cavity with the asymmetric cladding can be made as large or larger than the symmetric air-cladded structure if the semiconductor is made thick enough.

236 K

143 K

Ambient Temp. = 143 K

Figure 2.   Ave. Power of 7mW incident, 0.4% duty cycle

symmetric cladding

top

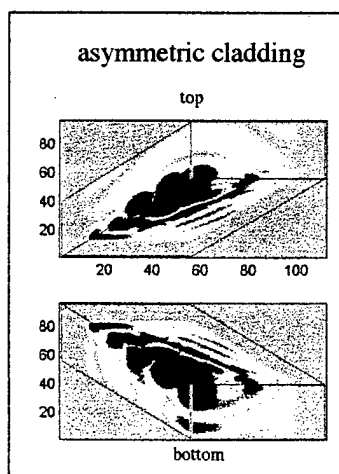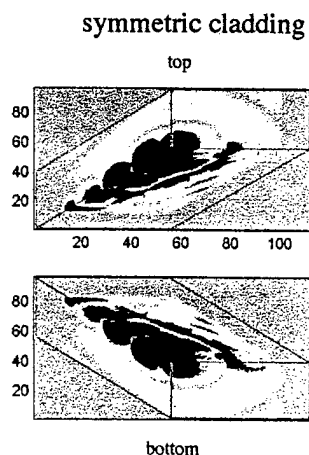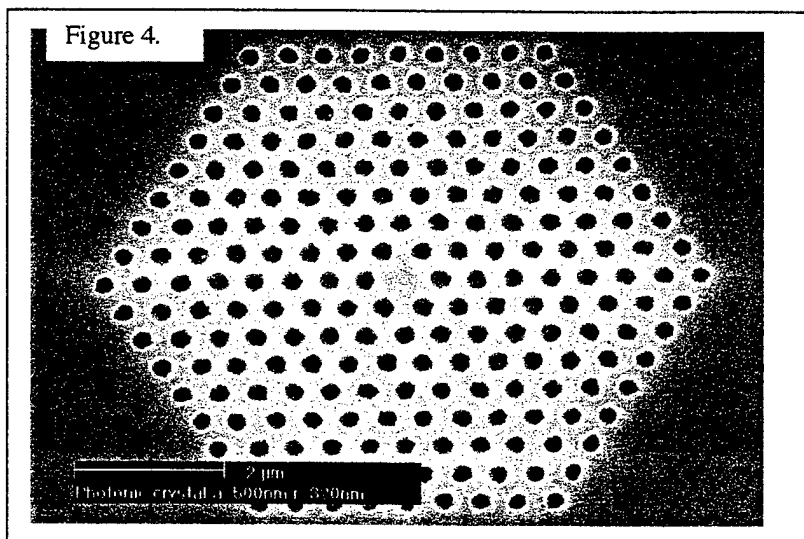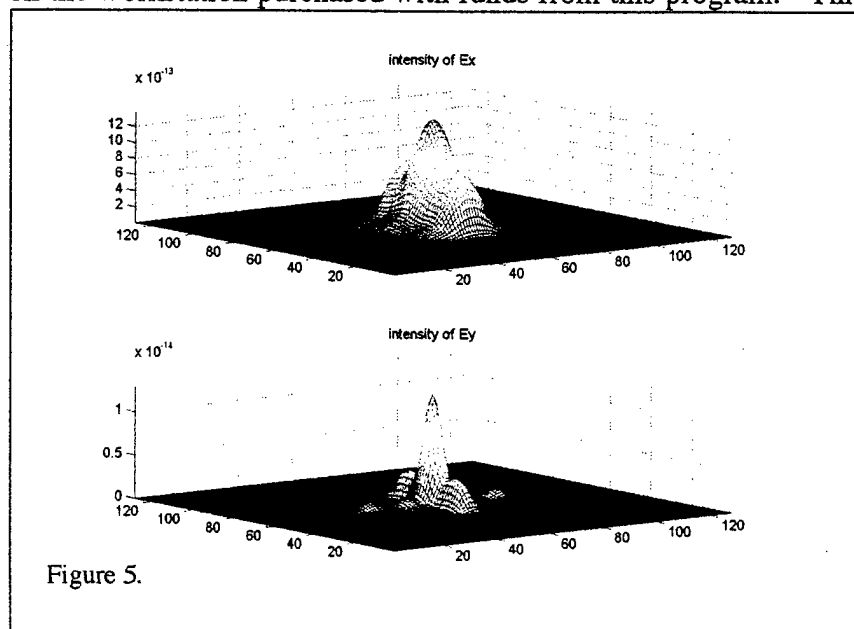asymmetric cladding

top

bottom

bottom

Figure 3.

Practically, the Q is limited by the obtainable etch depth. This will determine the maximum membrane thickness, and the vertical loss decreases with increasing semiconductor thickness.

Figure 4.

These microcavities are currently being fabricated here at USC. Shown below in figure 4 is an electron micrograph of an undercut membrane fabricated in my group. We are also collaborating with Professor Dapkus to fabricate photonic crystal microcavities with a far-field radiation pattern that has been engineered either to produce a linearly polarized circular beam, or to produce a fan-out pattern for free-space interconnections between electronics layers. This work is being supported by a DARPA STAB program and a DARPA WASSP program, respectively. In order to perform this engineering of the radiation field, we must be able to model this field. Shown below is a calculated radiation field for the microcavity laser demonstrated in [1-3]. This calculation was done in my group on the workstation purchased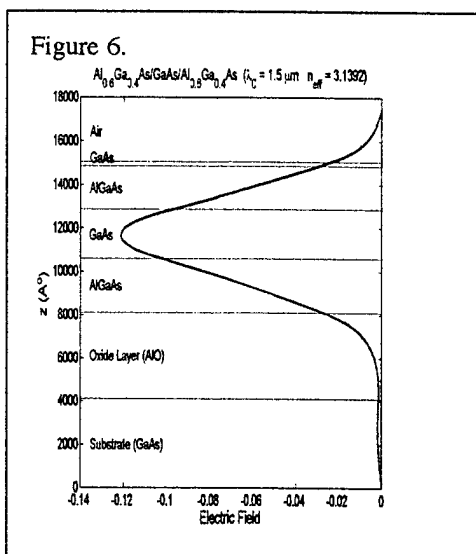 with funds from this program. This calculation was done by calculating the complex near-field by the finite-difference time-domain method. This field was then the input for a vector-diffraction theory calculation of the far-field. The figure illustrates that the x-component of the electric field is an order of magnitude larger that the y-component of the electric radiation

Figure 5.

4

field. This is in agreement with data taken at Caltech on the photonic crystal defect lasers.

The finite-difference time-domain calculations were written in C. These calculations can be very time-consuming so we have augmented the workstation purchased under this program with more workstations. The goal here is to use the multiple workstations to do these calculations in parallel. We are currently debugging this parallel version of the code.

We are also designing and fabricating photonic bandgap defined waveguides. Here, the waveguides are defined in a GaAs/AlGaAs slab-waveguide epitaxial structure. The layer structure is shown in figure 6. Below the bottom waveguide cladding is a layer of AlAs that will be converted to Al_xO_y by wet-oxidation. The purpose of this layer is to isolate the guided mode from the high-index substrate. Or, in other words, the AlO is included to guarantee that the waveguide mode is not a leaky mode. Here again we can do finite-difference time-domain calculations to model the waveguide. We are also considering other approaches to waveguide modeling. These other approaches include calculating both the reflectivity and the phase of the reflection coefficient. This works is based on the work of Sakoda in [4-5]. Once we have the complex reflection coefficient, we can construct the waveguide mode using a transverse-resonance scheme. An example of a fie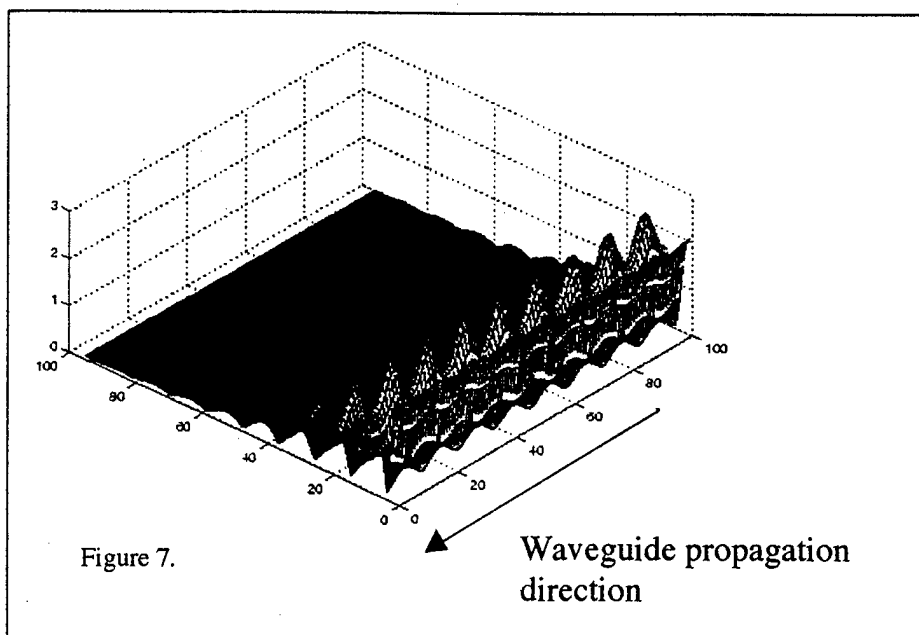ld calculated using this method is shown below in figure 7. In the figure, half of the field is shown. The other half is identical because of the symmetry. The drawback of this method is that it is a purely two-dimensional calculation. This method, then, is incapable of dealing with the critical issue of guided versus leaky mode behavior of these waveguides. We are also working

Figure 6.

Figure 7.   ▲   Waveguide propagation direction

on a finite-element code to calculate the eigenmodes of these structures directly. This has the advantage of eliminating the filtering routines that accompany solving for an eigenmode using the finite-difference time-domain algorithms. These calculations are also being done on the workstation purchased using funds from this program. Our goal is to do three-dimensional calculations of the photonic crystal waveguides.

We are also fabricating two-dimensional photonic crystal waveguides here at USC. This is done in collaboration with, and with support from, Agilent. Here the

Figure 8.
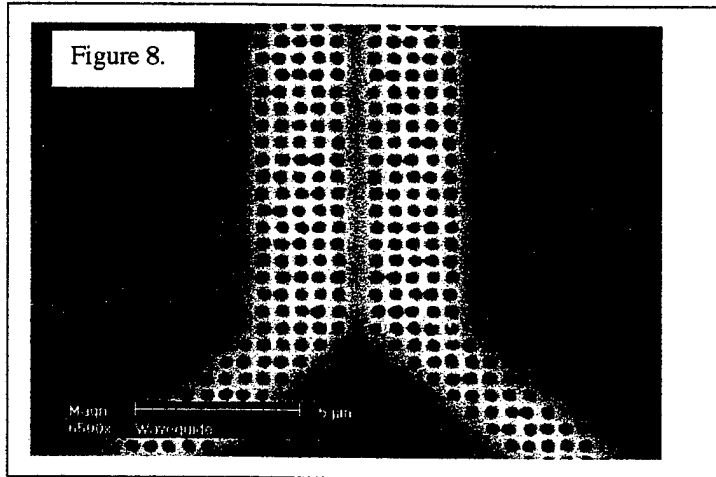
pattern transfer is very similar to that of the photonic crystal microcavities. The etching here at USC involves an Ar^+ ion beam mill, a reactive ion etch, and an electron cyclotron resonance system etch. In the ECR, the GaAs structures are etched with a BCl_3/Ar mixture, and the InP structures are etched with a CH_4/H_2/Ar recipe. This micrograph shows the input-coupling region. This is one of the programs for which the New Focus tunable laser was purchased. The laser complements an existing waveguide characterization setup in Professor Dapkus' lab. This setup is shared by the two research groups. The laser modules are controlled by an existing laser controller. Experimentally, we are interested in measuring the waveguide loss and in understanding the frequency range over which a guided mode exists.

Finally, we are also working on designing, fabricating, and characterizing structures that utilize the eigenstates of the periodic lattice for their functionality. In particular, we are working on the super-dispersion effects reported by NEC [6-7]. Here there is a program in collaboration with Professor Levi at USC funded by a DARPA STAB program. In these devices, the optical behavior is "built-in". The bandedge states are both spatially and spectrally dispersive. We are investigating both one-dimensional and two-dimensional periodic structures. In one-dimension, the analysis can be can be done nearly analytically. The eigenstates of the one-dimensionally periodic media can be solved using a matrix method [8]. Then to solve for the guided modes of the slab, we follow Russell, [9-10], and expand the periodic part of the Bloch functions in terms of spatial harmonics and keep only the first two terms. These are then matched to fields in the air cladding regions. Shown at right is the dispersion

Figure 9.

6
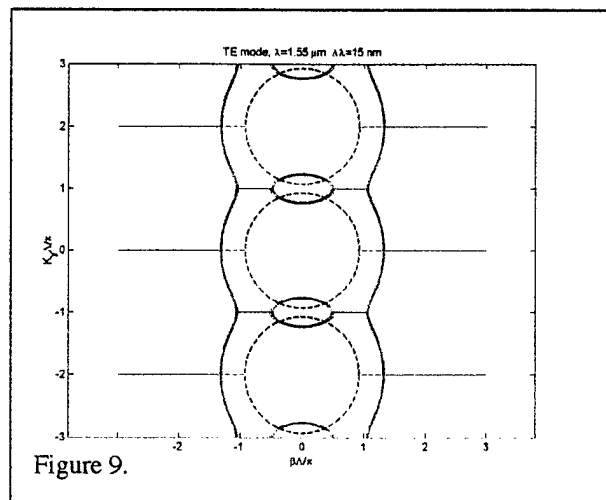
surface of the one-dimensional media. This curve is the dispersion surface for an infinite one-dimensional media. Near the Brillouin zone edge, there is a region where the desired dispersion occurs. This phenomenon has been understood for many years. See, for example, [11]. We are also interested in investigating this effect in two-dimensional structures. In two-dimensions, the dispersive region does not have to occur at the zone boundary. This gives increased freedom in designing the coupling angles. For these devices, the bandstructure is calculated using either a finite–difference time-domain procedure or a plane-wave basis bandstructure calculation. The finite-difference time-domain method starts with a field with a given k. This field is allowed to propagate before Fourier transforming the field to obtain the eigenfrequencies of the propagating modes. To obtain the bandstructure, the initial k is varied across the Brillouin zone. The figure shows a plane wave bandstructure calculation and constant frequency contours over a quarter of the Brillouin zone for a particular band. Since the group velocity is normal to the constant frequency contours in the direction of increasing frequency, it is clear that there are regions in this plot where the propagation direction is changing with frequency. We are planning to investigate the use of these structures for beamsteering as
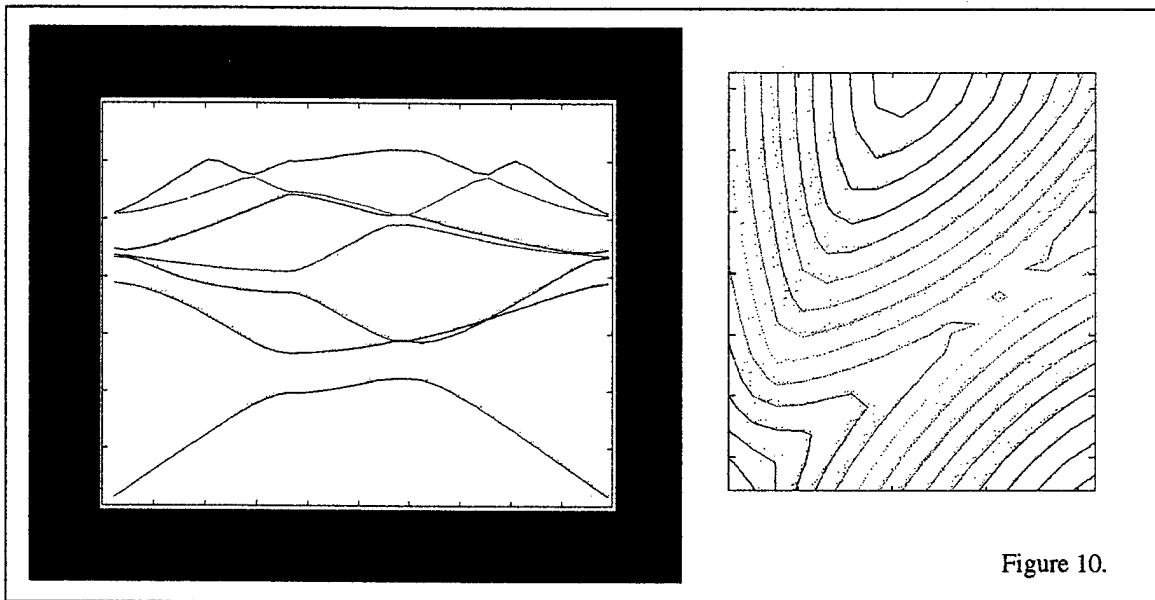

Figure 10.

well a s multiplexing and demultiplexing applications. As part of this investigation we are also interested in understanding how robust these structures are compared to device geometries that contain a defect guiding region. We are also very interested in understanding how to efficiently couple fields from non-photonic crystal media into photonic crystal media. As an example, the figure below shows a point source in free space radiating into a region in which the photonic crystal lattice constant is changing. Here we see a factor of 6 reduction in the reflectivity compared to a semiconductor interface, but this number has not been corrected for the reduced effective index in the periodically varying photonic crystal case.

Again, all of these calculations are being done with code written by my students on workstations in the lab. Finally, we are also beginning to fabricate these one-dimensional and two-dimensional periodic structures. Examples are shown in the micrographs below. In the one-dimensional case, the lines are 80 nm wide. Below that, is a two-dimensional lattice. The lithography is done on an SEM converted by my students to do lithography. The maximum pattern size is determined by the magnification of the microscope at which the pattern is written
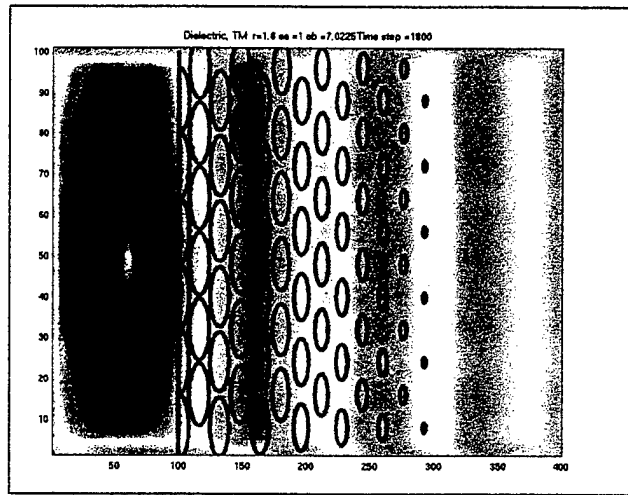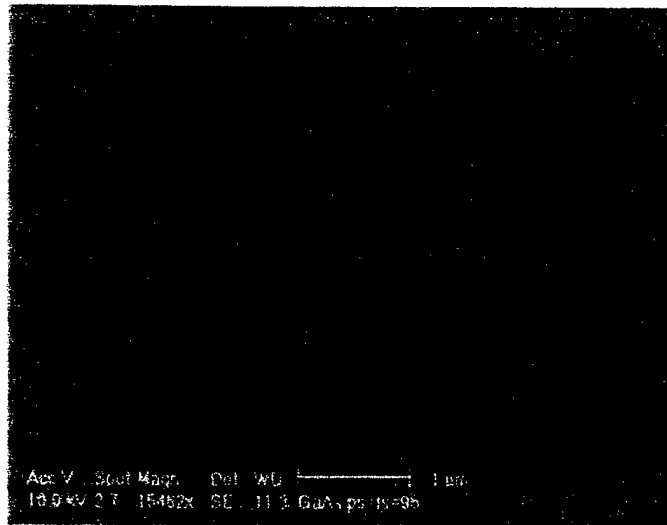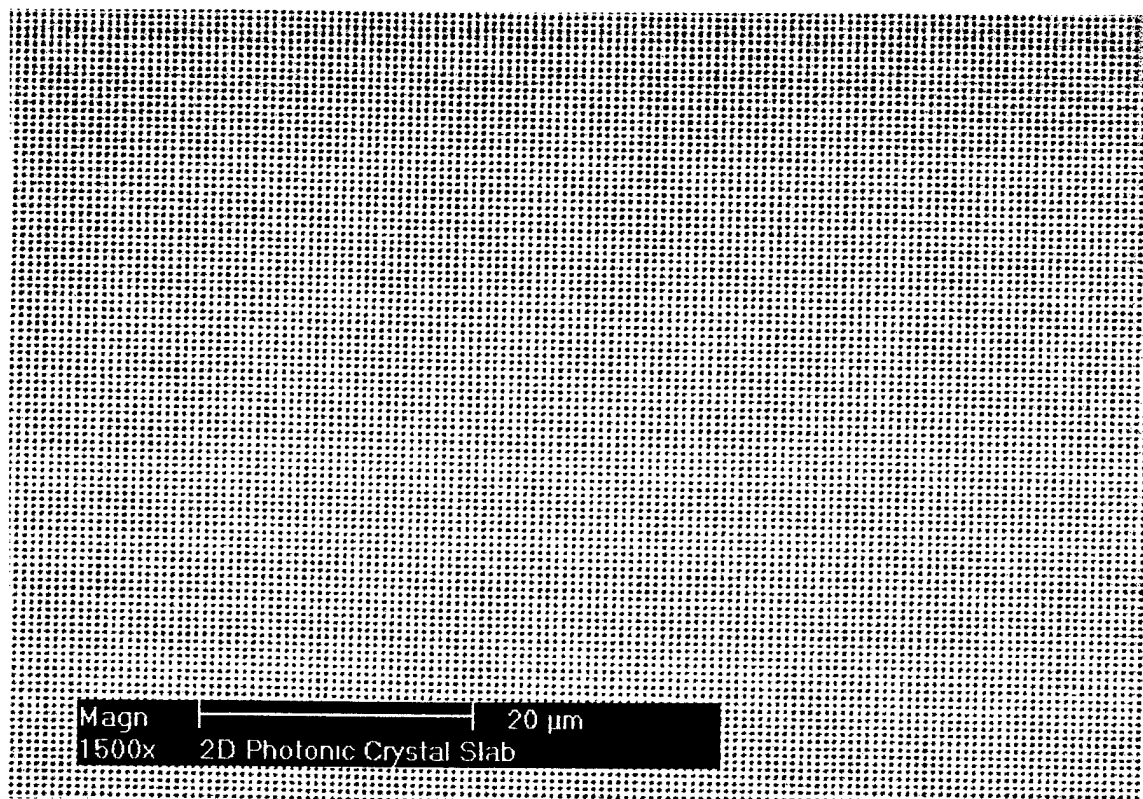

Figure 12.

Magn
1500x   2D Photonic Crystal Slab   20 µm

7. List of all participating scientific personnel
No graduate students were funded by this DURIP program, but the following graduate students have used the equipment purchased: Roshanak Shafiiha, Cheolwoo Kim, Woo Jun Kim, Andrew Stapleton, Po-Tsung Lee.

9. Bibliography

[1] O. Painter, R. K. Lee, A. Yariv, A. Scherer, J. D. O'Brien, P. D. Dapkus, I. Kim, "Two-Dimensional Photonic Crystal Defect Laser", *Science,* **284**, pp.1819-1821 (1999).

[2] O.J. Painter, A. Husain, A. Scherer, J.D. O'Brien, I. Kim, P.D. Dapkus, "Room Temperature Photonic Crystal Defect Lasers at Near-Infrared Wavelengths in InGaAsP", *IEEE J. Lightwave Tech.*, **17**, pp. 2082-2087 (1999).

[3] O. Painter, A. Husain, A. Scherer, P. Lee, I. Kim, J. D. O'Brien, P. D. Dapkus, "Lithographic Tuning of a Two-Dimensional Photonic Crystal Laser Array", *IEEE Phot. Tech. Lett.*, **12**, pp. 1126-1128 (2000).

[4] K. Sokoda, "Transmittance and Bragg reflectivity of two-dimensional photonic lattices", *Phys. Rev. B.*, **52**, pp. 8992-9002 (1995).

[5] K. Sakoda, "Optical transmittance of a two-dimensional triangular photonic lattice", *Phys. Rev. B.*, **51**, pp. 4672-4675 (1995).

[6] H. Kosaka, T. Kawashima, A. Tomita, M. Notomi, T. Tamamura, T. Saito, S. Kawakami, "Self-collimating phenomena in photonic crystals", *Appl. Phys. Lett.*, **74**, pp. 1212-1214 (1999).

[7] H. Kosaka, T. Kawashima, A. Tomita, M. Notomi, T. Tamamura, T. Sato, S. Kawakami, "Superprism phenomena in photonic crystals", *Phys. Rev. B.* **58**, pp. R10096-R10099 (1998).

[8] A. Yariv, P. Yeh, *Optical Waves in Crystals,* Wiley, 1984.

[9] P. St. J. Russell, "Optics of Floquet-Bloch Waves in Dielectric Coatings", *Appl. Phys. B.*, **39**, pp. 231-246 (1986).

[10] D. M. Atkin, P. St. J. Russell, T. A. Birks, P. J. Roberts, "Photonic band structure of guided Bloch modes in high index films fully etched through with periodic microstructure", *J. Mod. Opt.*, **43**, pp. 1035-1053 (1996).

[11] R. Zengerle, "Light propagation in singly and doubly periodic planar waveguides", *J. Mod. Opt.* , **34**, pp. 1589-1617 (1987).